Article

Discovery Medicine 2026; 38(208): 1570–1582
https://doi.org/10.24976/Discov.Med.202638208.123

Regulatory Mechanism of SREBP1-Mediated Lipid Metabolic Remodeling in Osteoclast Differentiation

Xiaojun Li[1], Bingjian Lin[1], Fayi Li[1], Nan Zhou[1,*]

[1]Department of Orthopaedics, The People's Hospital of Longgang, 325802 Wenzhou, Zhejiang, China
*Correspondence: chencheng26@126.com (Nan Zhou)
Submitted: 29 January 2026 Revised: 18 March 2026 Accepted: 2 April 2026 Published: 20 May 2026

Background: Sterol regulatory element-binding protein 1 (SREBP1) is a key regulator of lipid metabolism. However, its role in osteoclast differentiation and bone resorption remains unclear. This study investigated the function of SREBP1-mediated lipid metabolic remodeling in osteoporosis.

Methods: An ovariectomized (OVX) mouse model and SREBP1 conditional knockout mice were used to evaluate bone metabolism *in vivo*. RAW264.7 cells were stimulated with Receptor Activator of Nuclear Factor κB Ligand (RANKL) to induce osteoclast differentiation *in vitro*. Fatostatin and oleic acid were used to modulate SREBP1 activity and lipid metabolism.

Results: OVX mice showed significantly increased SREBP1 expression compared with the Control group ($p < 0.05$). Lipid synthesis enzymes Fatty Acid Synthase (FASN), Acetyl-CoA Carboxylase (ACC), and Stearoyl-CoA Desaturase 1 (SCD1) were also elevated ($p < 0.05$). Serum bone resorption markers C-terminal Telopeptide of Type I Collagen (CTX-I) and Tartrate-Resistant Acid Phosphatase (TRACP) were increased ($p < 0.05$), whereas bone formation markers Procollagen Type I N-terminal Propeptide (PINP) and Bone-specific Alkaline Phosphatase (B-ALP) were reduced ($p < 0.05$). These alterations were partially reversed in OVX+SREBP1 knockout mice ($p < 0.05$). *In vitro*, SREBP1 expression progressively increased during RANKL-induced osteoclast differentiation ($p < 0.05$). This increase correlated with elevated Nuclear Factor of Activated T Cells 1 (NFATC1), Tartrate-Resistant Acid Phosphatase (TRAP), and Cathepsin K (CTSK) expression ($p < 0.05$). Fatostatin significantly reduced osteoclast formation and bone resorption activity ($p < 0.05$), and suppressed lipid metabolism enzyme expression ($p < 0.05$). Oleic acid supplementation partially restored osteoclast differentiation and function ($p < 0.05$).

Conclusion: SREBP1 promotes osteoclast maturation and bone resorption by regulating lipid metabolism. Targeting SREBP1 or modulating fatty acid metabolism may provide a potential therapeutic strategy for osteoporosis.

Keywords: SREBP1; lipid metabolism; osteoclast differentiation; bone resorption; osteoporosis

Introduction

Bone remodeling is a dynamic and tightly regulated process orchestrated by the coordinated actions of osteoblasts and osteoclasts. Disruption of this balance is a pivotal event in the pathogenesis of metabolic bone disorders such as osteoporosis. Osteoclast differentiation and activity are primarily governed by the Receptor Activator of Nuclear Factor κB Ligand (RANKL)/Macrophage Colony-Stimulating Factor (M-CSF) signaling pathway. The transcription factor Nuclear Factor of Activated T Cells 1 (NFATC1) serves as the master regulator of osteoclastogenesis by directly activating effector genes such as Tartrate-Resistant Acid Phosphatase (TRAP) and Cathepsin K, thereby mediating matrix degradation and bone resorption. The molecular framework of this canonical signaling axis has been extensively characterized [1,2].

In addition to classical signaling cascades, metabolic reprogramming has emerged as a critical regulatory layer in immune and myeloid cell function. Among various metabolic pathways, lipid metabolism plays a central role in macrophage/osteoclast lineage commitment and effector activity. Fatty acids and cholesterol not only provide structural and energetic substrates but also act as signaling mediators that modulate transcriptional networks and receptor activation, thereby influencing cell fusion, lysosomal enzyme secretion, and bone resorption capacity [3–5]. Dynamic alterations in lipid metabolism-related enzymes during osteoclastogenesis further support a functional link between lipid metabolic remodeling and bone homeostasis [6,7].

The sterol regulatory element-binding protein (SREBP) family functions as a master regulator of lipid biosynthesis by transcriptionally controlling genes involved in fatty acid and cholesterol synthesis. Pharmacological inhibition of SREBPs has demonstrated therapeutic potential in metabolic and inflammatory disorders [8–10]. In bone metabolism, previous studies have reported that SREBP inhibition suppresses RANKL-induced osteoclast differentiation and attenuates bone loss in animal models [11,12]. Given that fatty acid composition critically

influences membrane dynamics, energy metabolism, and lipid-derived signaling molecules, Sterol regulatory element-binding protein 1 (SREBP1) may exert distinct regulatory effects on osteoclast differentiation compared with SREBP2 [13]. Despite emerging evidence implicating SREBP signaling in bone metabolism, whether SREBP1-mediated fatty acid metabolic reprogramming directly modulates osteoclastogenesis has not been systematically investigated. This gap represents a key unresolved question in understanding lipid-bone crosstalk [14].

The biological effects of fatty acids on osteoclasts are bidirectional and depend on their type and the degree of saturation. Saturated fatty acids may promote osteoclast formation, whereas certain monounsaturated fatty acids can suppress osteoclast activity through modulation of transcriptional programs [15–17]. These findings suggest that endogenous fatty acid synthesis controlled by SREBP1 may influence osteoclast phenotypes not only quantitatively but also qualitatively through compositional remodeling. In ovariectomy (OVX)-induced osteoporosis models, systemic lipid metabolism is significantly altered, and OVX has been reported to modulate SREBP1 expression in peripheral tissues [4,18]. However, it remains unclear whether SREBP1-dependent lipid metabolic changes in osteoclasts contribute directly to estrogen deficiency-induced bone loss [19].

Based on these observations, we hypothesized that SREBP1-driven fatty acid metabolic remodeling functions as a critical metabolic checkpoint in osteoclast differentiation and that disruption of SREBP1 signaling may attenuate pathological bone resorption by altering intracellular fatty acid composition. To test this hypothesis, we employed both genetic and pharmacological strategies, integrating *in vivo* and *in vitro* models to evaluate the role of SREBP1 in osteoclastogenesis and bone loss. Fatty acid profiling combined with exogenous oleic acid supplementation was further conducted to determine whether compositional changes in fatty acids mediate the functional effects of SREBP1 deficiency, thereby providing isoform-specific mechanistic evidence for SREBP1 as a potential therapeutic target in metabolic bone diseases.

Materials and Methods

Animals

Female C57BL/6 mice (6–8 weeks old, SPF grade) were obtained from Speifu Biotechnology Co., Ltd. (Beijing, China). Conditional *SREBP1*$^{fl/fl}$ mice were generated on a C57BL/6J background using CRISPR/Cas9 technology by Nanjing GemPharmatech Co., Ltd. All animals were maintained under specific pathogen-free (SPF) conditions with controlled temperature and humidity, a 12-hour light/dark cycle, and ad libitum access to food and water.

Animal Grouping and Establishment of the Ovariectomy Model

All animal experiments were approved by the Animal Ethics Committee of South Zhejiang Institute of Radiation Medicine and Nuclear Technology Applications (ZFY20250896). Twenty female mice (8 weeks old) were randomly assigned to four groups (n = 5 per group): Control, OVX, KO-SREBP1, and OVX+KO-SREBP1. SREBP1 conditional knockout mice were generated using a Cre-loxP system in which SREBP1 was specifically deleted in osteoclast-lineage cells under the control of Ctsk-Cre. Wild-type littermates served as controls [20]. The OVX model was established using a standard bilateral ovariectomy procedure under sodium pentobarbital anesthesia (50 mg/kg) [21]. The Control and KO-SREBP1 groups underwent identical surgery without ovary removal. The modeling period lasted eight weeks [22]. Model success was confirmed by impaired bone mechanical properties, increased TRAP-positive osteoclasts, trabecular deterioration in histology, and elevated serum C-terminal Telopeptide of Type I Collagen (CTX-I) and Tartrate-Resistant Acid Phosphatase (TRACP) levels. The modeling success rate exceeded 90%. At the endpoint, mice were euthanized by carbon dioxide inhalation followed by cervical dislocation. Femurs and tibiae were collected for subsequent analyses.

Body Weight and Behavioral Testing

Body weight was recorded weekly throughout the experimental period. At week 8, an exercise endurance test using a running wheel was performed to evaluate the overall improvement in osteoporotic phenotype.

Three-Point Bending Test

After sacrifice, the left tibia was dissected, cleaned of surrounding soft tissues, wrapped in saline-soaked gauze, and stored at –80 °C until mechanical testing (within one month). Before testing, the bones were thawed to room temperature and subjected to a three-point bending test using a CellScale Univert system (CellScale, Waterloo, Canada) with an 8 mm span and a loading rate of 0.1 mm/s until fracture occurred. Load-displacement curves were recorded, and maximum load (N), stiffness (N/mm), fracture energy (N·mm), and Young's modulus (MPa) were calculated using the instrument's software.

Histological Analysis

Femora were decalcified in 10% EDTA (HY-Y0682, Sigma-Aldrich, MO, USA, pH 7.4) for 1 month, with the decalcifying solution refreshed every 2 days. After decalcification, samples were dehydrated in graded ethanol (459828, Sigma-Aldrich), cleared in xylene (534056, Sigma-Aldrich), and embedded in paraffin. Sections (5 µm thick) were prepared and stained with hematoxylin-eosin (HE; C0105S, Beyotime, Shanghai, China) and Masson's trichrome (HT15, Sigma-Aldrich, MI, USA) accord-

ing to the manufacturer's instructions. Tartrate-resistant acid phosphatase (TRAP) staining was performed using a commercial kit (G1492, Solarbio, Beijing, China) according to the manufacturer's instructions. Positive staining was identified as bright red or dark red granules localized in the cytoplasm. TRAP-positive cells along the trabecular bone surface were observed under a light microscope (Olympus, Tokyo, Japan).

Serum Biochemical Analysis

Serum samples were collected, and Enzyme-Linked Immunosorbent Assay (ELISA) kits were used to measure bone resorption markers, including CTX-I (JL20123, JONLNBIO, Shanghai, China) and TRACP (JL11586, JONLNBIO), as well as bone formation markers Procollagen Type I N-terminal Propeptide (PINP, JL20174, JONLNBIO) and Bone-specific Alkaline Phosphatase (B-ALP, JL20367, JONLNBIO), to assess systemic bone metabolic balance.

Cell Culture and Induction

RAW264.7 macrophages (SNL-112, SUNNCELL, Wuhan, China) were used as an *in vitro* model for osteoclast differentiation. Cells were cultured in Dulbecco's Modified Eagle's Medium (DMEM, Thermo Fisher Scientific #12491015, Waltham, MA, USA) supplemented with 10% fetal bovine serum (Thermo Fisher Scientific #A5256701) and 1% penicillin-streptomycin (Thermo Fisher Scientific #15140122). The cell line was authenticated by the supplier using short tandem repeat (STR) profiling. Routine mycoplasma testing was performed with a PCR-based detection kit, and all cultures were confirmed to be mycoplasma-free before experiments. In addition, no evidence of chlamydia contamination was detected according to the supplier's quality control report. Differentiation was induced by adding 100 ng/mL recombinant mouse RANKL (ab307187, Abcam, Cambridge, UK) [23], and cells were collected at days 0, 1, 3, and 5 for subsequent analyses.

Establishment and Grouping of the In Vitro Model

RAW264.7 precursor cells were seeded into 24-well plates at a density of 1×10^4 cells per well and allowed to adhere before the application of the different treatments. Cells in the control group were induced to differentiate with 100 ng/mL RANKL alone. In the Fatostatin group, 30 µM Fatostatin (HY-14452, Sigma-Aldrich, MO, USA) was added in combination with RANKL to inhibit SREBP1 signaling. In the Fatostatin + OA group, 100 µM oleic acid [24] (364525, Sigma-Aldrich, MO, USA) was supplemented with 100 ng/mL RANKL and 30 µM Fatostatin to restore lipid metabolism through exogenous fatty acid supplementation. The induction period lasted for 5–6 days, during which the fresh medium containing the indicated treatments was replaced every two days until multinucleated osteoclasts were formed.

TRAP Staining

RAW264.7 cells were seeded at 1×10^4 cells/well in 24-well plates. After treatment, cells were washed with PBS and fixed in 4% paraformaldehyde for 20 min at room temperature. TRAP staining was performed using a commercial kit (G1492, Solarbio, Beijing, China), which utilizes a red chromogenic substrate for the detection of TRAP activity, according to the manufacturer's instructions. TRAP-positive multinucleated cells containing three or more nuclei were identified as osteoclasts. Images were captured under a light microscope (Olympus, Tokyo, Japan). TRAP-positive osteoclasts were counted in five randomly selected fields per well, and the average number of osteoclasts per field was calculated and used for statistical analysis.

Measurement of Collagen Type I Degradation Product (CTX-I)

A total of 2×10^5 cells were seeded on bone slices and cultured for 3 days, followed by replacement with acidified medium (pH 6.5, adjusted with 0.085% HCl) with or without 10 ng/mL RANKL. After 6 days, supernatants were collected, and CTX-I levels were measured using an ELISA kit to reflect osteoclastic bone resorption activity. Fifty microliters of each sample were analyzed, and background values from blank bone slices and medium were subtracted.

Cathepsin K Activity Assay

RAW264.7 cells (5×10^5 cells/well) were seeded in 6-well plates and stimulated with RANKL for 6 days. Cathepsin K activity was measured using a commercial assay kit (ab65303, Abcam, Cambridge, UK). Cells were lysed on ice in 200 µL of lysis buffer for 10 min, and lysates were centrifuged at 14,000 ×g for 5 min. Protein concentrations were determined using a BCA protein assay (PI23225, Thermo Fisher Scientific, Waltham, MA, USA). Fifty microliters of lysate containing 3 µg of total protein were added to a 96-well plate, and the reaction mixture was incubated at 37 °C for 2 h. Fluorescence intensity (excitation 355 nm, emission 520 nm) was measured using a microplate reader (iMark™, Bio-Rad Laboratories, Hercules, CA, USA) to assess enzyme activity.

Cell Counting Kit-8 (CCK-8) Assay for Cell Viability

CCK-8 assay was performed to assess the viability of RAW264.7 cells after Fatostatin treatment. RAW264.7 cells were seeded in 96-well plates at a density of 5×10^3 cells/well and allowed to adhere overnight. Cells were then treated with 0, 10, 20, 30, or 40 µM Fatostatin for 48 h. At the end of treatment, 10 µL of CCK-8 solution (ab228554, Abcam, Cambridge, UK) was added to each well and incubated at 37 °C for 2 h. Absorbance at 450 nm was measured using a Bio-Rad iMark™ microplate reader (Bio-Rad Laboratories, Hercules, CA, USA). Cell viability was calculated relative to the control group, and experiments were performed in triplicate.

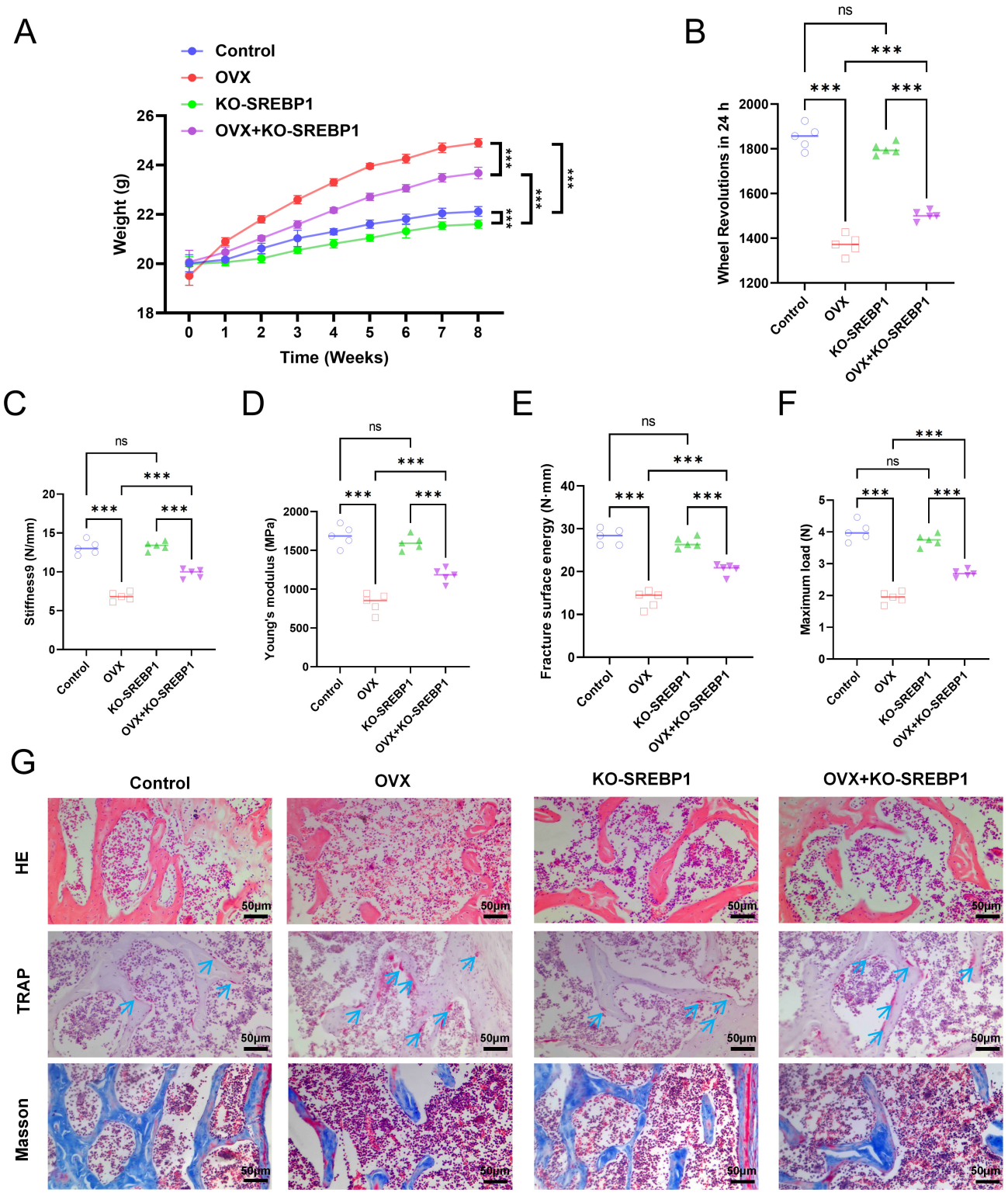

Fig. 1. Physiological parameters and femoral histology in mice. (A) Body weight changes. (B) 24-hour running wheel distance. (C–F) Tibial stiffness, Young's modulus, fracture surface energy, and maximum load. (G) HE, TRAP, and Masson staining of femoral sections. Blue arrows indicate positive cells. n = 5; ns, $p > 0.05$; ***$p < 0.001$. HE, Hematoxylin and Eosin.

Western Blot Analysis

Total proteins were extracted from mouse bone marrow cells and differentiated RAW264.7 cells using RIPA lysis buffer. Protein concentrations were quantified with a BCA assay (23225, Thermo Fisher Scientific, Shanghai, China). Equal amounts (20–30 μg) of protein were separated by SDS-PAGE and transferred to PVDF membranes

Table 1. Primary antibodies for Western blot analysis.

Antibody	Brand	Catalog number	Dilution ratio
SREBP1	Abcam, Cambridge, UK	ab313881	1:1000
FASN	Abcam	ab128870	1:10,000
ACC	Abcam	ab45174	1:1000
SCD1	Abcam	ab236868	1:1000
NFATC1	Proteintech, Wuhan, China	66963-1-Ig	1:1000
TRAP	Abcam	ab52750	1:5000
CTSK	Abcam	ab187647	1:1000
RANK	Abcam	ab200369	1:500
GAPDH	Proteintech	60004-1-Ig	1:5000

SREBP1, Sterol Regulatory Element-Binding Protein 1; FASN, Fatty Acid Synthase; ACC, Acetyl-CoA Carboxylase; SCD1, Stearoyl-CoA Desaturase 1; NFATC1, Nuclear Factor of Activated T Cells 1; TRAP, Tartrate-Resistant Acid Phosphatase; CTSK, Cathepsin K; RANK, Receptor Activator of Nuclear Factor κB; GAPDH, Glyceraldehyde-3-Phosphate Dehydrogenase.

(WJ002S, Epizyme, Shanghai, China). Membranes were blocked with protein-free rapid blocking buffer (PS108P, Epizyme) for 15 min at room temperature, and incubated overnight at 4 °C with primary antibodies (listed in Table 1). After washing three times with TBST, membranes were incubated for 1 h at room temperature with HRP-conjugated secondary antibodies: goat anti-rabbit IgG-HRP (ab6721, Abcam, 1:2000) and goat anti-mouse IgG-HRP (ab205719, Abcam, 1:2000). After three additional PBST washes (P3563-10PAK, Merck, Darmstadt, Germany), protein bands were visualized using enhanced chemiluminescence (ECL) reagents (BL520A, BioSharp, Hefei, China) and imaged with a Bio-Rad ChemiDoc XRS+ system (Bio-Rad, Hercules, CA, USA). Band intensities were quantified using ImageJ Pro Plus 6.0 software (Media Cybernetics, Rockville, MD, USA). The expression levels of target proteins were normalized to the corresponding internal control protein (GAPDH), and the relative protein expression levels were calculated for statistical analysis.

Statistical Analysis

All data are presented as mean ± Standard Error of the Mean (SEM). Statistical analyses were performed using GraphPad Prism 7.0 (GraphPad Software, San Diego, CA, USA). Prior to parametric analysis, data were tested for normality using the Shapiro-Wilk test and for homogeneity of variance using Levene's test. For normally-distributed data that satisfied equal variance assumptions, differences between groups were evaluated using two-way Analysis of Variance (ANOVA) followed by Tukey's post hoc test. If the assumptions of normality or homogeneity of variance were violated, nonparametric tests were applied accordingly. Statistical significance was defined as $*p < 0.05$, $**p < 0.01$, $***p < 0.001$, and ns (not significant).

Results

Establishment and Evaluation of the Osteoporotic Mouse Model

In the Control group, mice maintained stable body weight and exercise endurance, and tibial mechanical parameters—including stiffness, Young's modulus, fracture energy, and maximum load—remained within normal ranges (Fig. 1A–F). Compared with the Control group, OVX mice showed significantly increased body weight and reduced 24-hour running distance (Fig. 1A,B). Tibial stiffness, Young's modulus, fracture energy, and maximum load were significantly decreased (Fig. 1C–F, $p < 0.05$). Histological staining revealed increased TRAP-positive osteoclasts and widened trabecular spacing (Fig. 1G). In the KO-SREBP1 group, body weight showed a slightly lower increase compared with Control (Fig. 1A), while exercise performance and tibial mechanical parameters remained comparable (Fig. 1B–F, $p > 0.05$), indicating that SREBP1 deficiency has limited effects on bone mechanics under physiological conditions. Importantly, OVX+KO-SREBP1 mice exhibited significantly improved mechanical parameters compared with OVX mice, including higher stiffness, fracture energy, and maximum load (Fig. 1C–F, $p < 0.05$). Running distance was partially restored (Fig. 1B, $p < 0.05$).

Histological analysis was performed to assess trabecular structure and collagen organization. HE staining showed that Control and KO-SREBP1 mice maintained regular and dense trabecular architecture, whereas OVX mice exhibited reduced trabecular number, thinner trabeculae, and increased marrow space. OVX+KO-SREBP1 mice showed partial recovery of trabecular structure compared with OVX mice (Fig. 1G). Masson staining revealed dense and well-organized collagen fibers in the Control and KO-SREBP1 groups, disorganized and sparse collagen in OVX mice, and improved collagen alignment in OVX+KO-SREBP1 mice (Fig. 1G). TRAP staining demonstrated fewer osteoclasts in

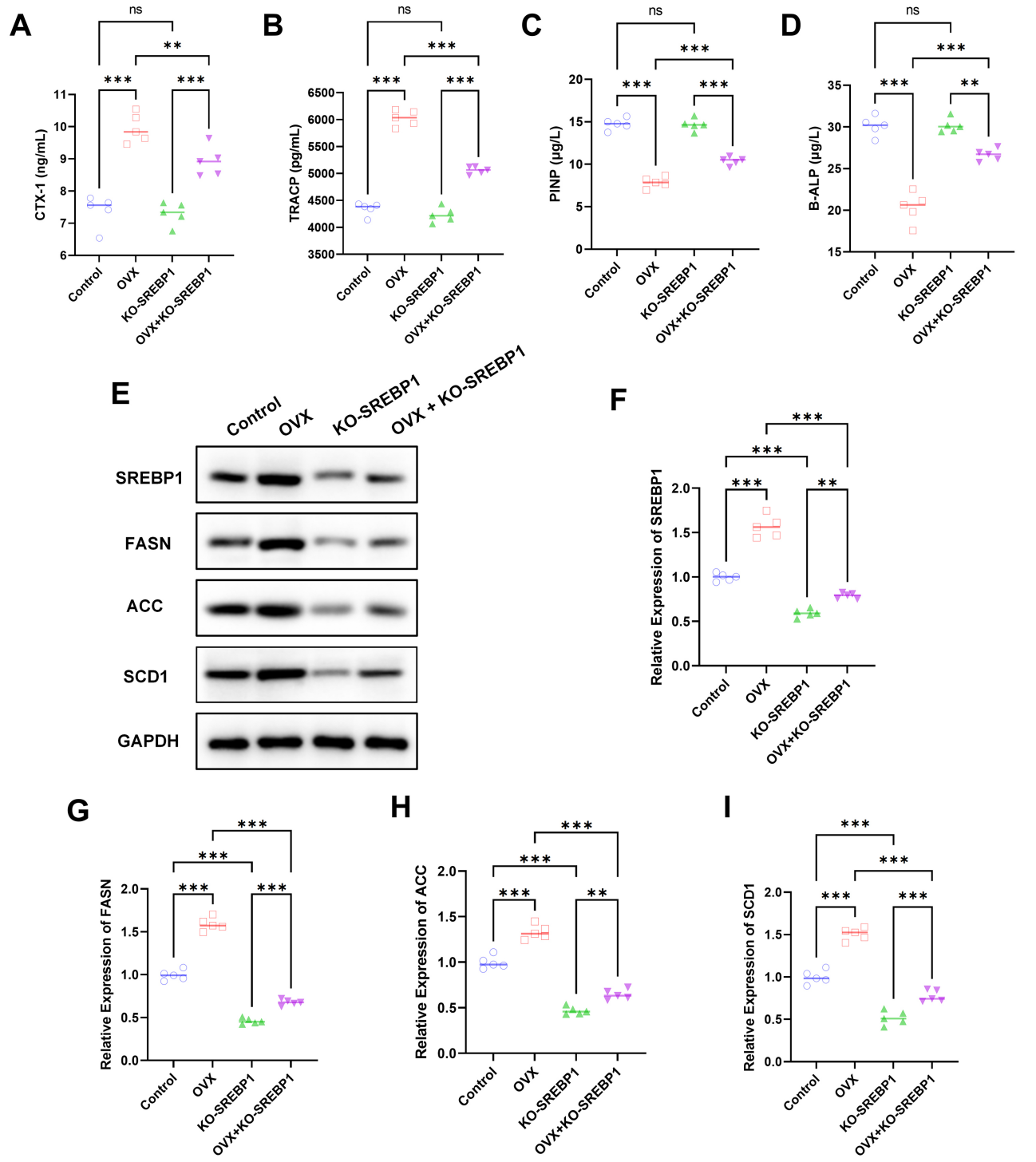

Fig. 2. Serum biochemical markers and bone marrow protein expression in mice. (A–D) ELISA analysis of CTX-I, TRACP, PINP, and B-ALP in serum. (E–I) Western blot analysis and densitometry of SREBP1 and lipid metabolism-related proteins FASN, ACC, and SCD1. n = 5; ns, $p > 0.05$; **$p < 0.01$; ***$p < 0.001$. ELISA, Enzyme-Linked Immunosorbent Assay; CTX-I, C-terminal Telopeptide of Type I Collagen; TRACP, Tartrate-Resistant Acid Phosphatase; PINP, Procollagen Type I N-terminal Propeptide; B-ALP, Bone-specific Alkaline Phosphatase.

Control and KO-SREBP1 mice, increased TRAP-positive osteoclasts in OVX mice, and a reduction in osteoclast numbers in OVX+KO-SREBP1 mice, consistent with the improvements in trabecular structure and collagen organization (Fig. 1G). These results indicate that SREBP1 deletion partially alleviates OVX-induced deterioration of bone mechanical properties and excessive osteoclast activation.

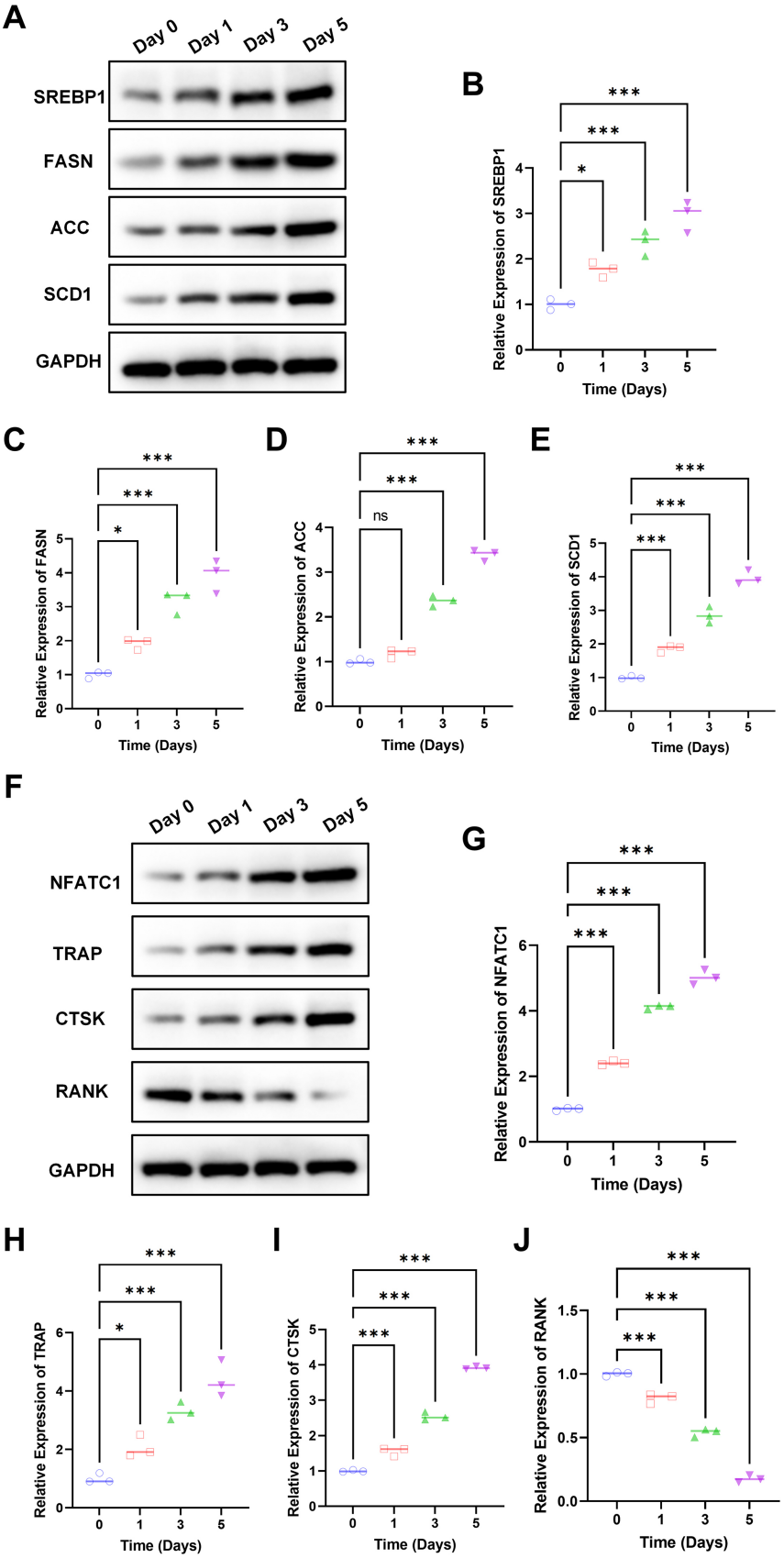

Fig. 3. Protein expression during osteoclast differentiation at days 0, 1, 3, and 5. (A–E) Western blot analysis and densitometry of SREBP1, FASN, ACC, and SCD1. (F–J) Western blot analysis and densitometry of NFATC1, TRAP, CTSK, and RANK. n = 3; ns, $p > 0.05$; *$p < 0.05$; ***$p < 0.001$.

In Vivo Investigation of SREBP1 Regulation on Osteoclast Differentiation

Serum ELISA results showed that OVX mice had significantly elevated bone resorption markers CTX-I and TRACP (Fig. 2A,B, $p < 0.05$), while bone formation markers PINP and B-ALP were decreased (Fig. 2C,D, $p < 0.05$), consistent with the observed reduction in bone mass and mechanical properties. In the KO-SREBP1 group, serum CTX-I, TRACP, PINP, and B-ALP levels were comparable to the Control group (Fig. 2A–D, $p > 0.05$), suggesting minimal effects under normal conditions. In OVX+KO-SREBP1 mice, CTX-I and TRACP levels were significantly lower than those in OVX mice, whereas PINP and B-ALP levels were partially restored (Fig. 2A–D, $p < 0.05$).

Western blot analysis demonstrated that SREBP1, FASN, ACC, and SCD1 were markedly upregulated in OVX bone marrow cells (Fig. 2E–I, $p < 0.05$). KO-SREBP1 mice showed reduced expression compared with the Control group, and OVX+KO-SREBP1 mice displayed significantly lower levels than OVX mice (Fig. 2E–I, $p < 0.05$). These data suggest that SREBP1 regulates osteoclast activation and bone resorption through modulation of lipid metabolism pathways.

Dynamic Expression of Proteins During Osteoclast Differentiation

To explore the temporal changes of SREBP1 during osteoclast differentiation, RAW264.7 cells were sampled at days 0, 1, 3, and 5 after RANKL induction. SREBP1 and its downstream targets FASN, ACC, and SCD1 showed a gradual increase over time and exhibited the highest levels at day 5 among the examined time points ($p < 0.05$, Fig. 3A–E). Similarly, osteoclast-specific markers NFATC1, TRAP, and CTSK were progressively upregulated, whereas RANK expression decreased over time ($p < 0.05$, Fig. 3F–J). These findings suggest that activation of the SREBP1 pathway is temporally associated with osteoclast differentiation and may contribute to metabolic adaptation during this process.

Regulation of Osteoclast Bone Resorption by SREBP1-Mediated Lipid Metabolism Remodeling

To investigate whether inhibition of SREBP1 affects osteoclast function, Fatostatin was used to suppress SREBP1 activity, with exogenous oleic acid (OA) added to restore lipid metabolism. Cell viability assessed by CCK-8 showed that 0–30 μM Fatostatin did not significantly affect RAW264.7 cell survival, whereas 40 μM Fatostatin markedly reduced cell viability (Fig. 4A; $p < 0.05$), indicating potential cytotoxicity at the highest dose. Therefore, subsequent functional analyses were performed using concentrations up to 30 μM.

Compared with the control group, Fatostatin treatment significantly reduced CTX-I levels and Cathepsin K activity in culture supernatants (Fig. 4B,C; $p < 0.05$), indicating impaired bone resorption capacity, whereas supplementation with oleic acid partially restored both CTX-I and Cathepsin K activity, suggesting that restoration of fatty acid metabolism can rescue osteoclast resorption function (Fig. 4B,C; $p < 0.05$). Western blot analysis confirmed that Fatostatin markedly decreased SREBP1 expression, along with reduced levels of lipid metabolism-related proteins FASN, ACC, and SCD1 (Fig. 4D–H; $p < 0.05$). Importantly, OA supplementation partially restored the expression of these proteins and improved resorption activity. These results indicate that pharmacological inhibition of SREBP1 suppresses osteoclast bone resorption, which can be partially rescued by restoring fatty acid metabolism.

Validation of SREBP1-Mediated Lipid Metabolism Remodeling in Osteoclast Differentiation

To further examine the effect of SREBP1 inhibition on osteoclast differentiation, TRAP staining and protein expression analyses were performed. Fatostatin treatment significantly reduced the number of TRAP-positive multinucleated osteoclasts (Fig. 5A,B; $p < 0.05$). OA supplementation partially restored osteoclast formation. Western blot analysis showed that Fatostatin decreased the expression of osteoclast differentiation markers NFATC1, TRAP, and CTSK, while RANK expression was increased (Fig. 5C–G; $p < 0.05$). These changes were partially reversed by OA supplementation. Taken together, these findings suggest that pharmacological inhibition of SREBP1 suppresses osteoclast differentiation and activation, and that restoration of lipid metabolism can partially rescue this inhibitory effect.

Discussion

This study demonstrates that SREBP1-mediated lipid metabolic remodeling plays an essential role in osteoclast differentiation and bone resorption. Here, we discuss our findings in the context of lipid metabolism, osteoclast regulation, fatty acid composition, estrogen deficiency, underlying mechanisms, and potential clinical implications.

Lipid Metabolism and Bone Remodeling

Lipid metabolism has emerged as an active regulator of bone remodeling beyond classical osteoblastic and osteoclastic signaling. Accumulation of fatty acids and other neutral lipids in bone marrow is negatively correlated with bone mineral density and structural integrity [25,26]. Lipid metabolites influence the balance between osteoblasts and osteoclasts, affecting osteoporosis progression [27]. In the context of osteoclasts, alterations in the expression of lipid metabolism-related enzymes or lipid receptors have been reported to affect differentiation and activity [3,28]. In line with these reports, OVX mice in our study showed elevated bone resorption markers and reduced mechanical properties (Fig. 1), accompanied by upregulation of SREBP1 and lipid metabolic proteins (Fig. 2), highlight-

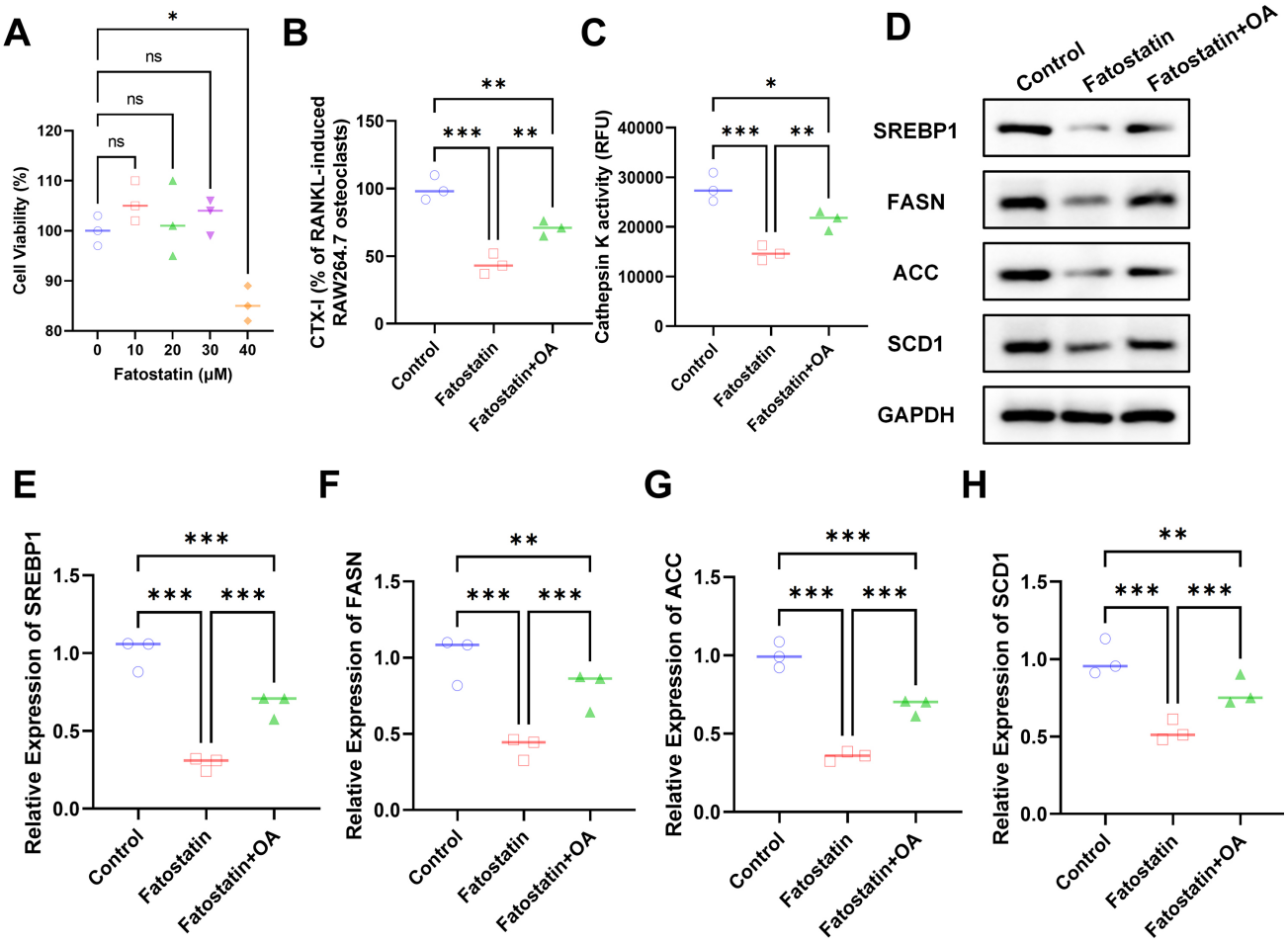

Fig. 4. Osteoclast bone resorption activity and associated protein expression. (A) CCK-8 assay showing cell viability after treatment with 0, 10, 20, 30, or 40 μM Fatostatin for 48 h. (B) CTX-I concentration in culture medium. (C) Cathepsin K activity. (D–H) Western blot analysis and densitometry of SREBP1, FASN, ACC, and SCD1. n = 3; ns, $p > 0.05$; *$p < 0.05$; **$p < 0.01$; ***$p < 0.001$. CCK-8, Cell Counting Kit-8.

ing a link between lipid dysregulation and bone loss. Intracellular lipid composition was not directly measured in this study. Therefore, lipid metabolic remodeling was inferred from changes in lipid metabolism–related proteins rather than direct lipidomic evidence. Future studies incorporating targeted or retrospective lipidomic analysis are warranted to validate these changes.

Regulatory Role of SREBP1 in Osteoclasts

SREBP1 is a key transcription factor regulating fatty acid synthesis and membrane lipid generation, with extensive studies in liver, adipose tissue, and skeletal muscle metabolism [29,30]. Its role in osteoclasts, however, has not been systematically explored. Previous studies primarily focused on SREBP2, showing that SREBP2 deficiency accelerates osteoclastogenesis and bone loss [12,31]. Here, SREBP1 and its downstream lipid metabolic targets were upregulated in OVX bone marrow and RANKL-induced RAW264.7 osteoclasts (Fig. 3). Pharmacological inhibition with Fatostatin suppressed osteoclast formation and resorptive activity (Figs. 4,5), indicating a positive regulatory role of SREBP1 in osteoclast differentiation and function. This provides a novel perspective for targeting SREBP1 in bone metabolism, contrasting with prior reports that RXR activation upregulates SREBP1c to inhibit osteoclasts [5].

Effects of Fatty Acid Composition on Osteoclast Function

Lipid metabolism involves not only overall lipid levels but also fatty acid chain length, degree of unsaturation, and metabolic enzyme activity. Saturated fatty acids promote osteoclastogenesis, whereas specific unsaturated fatty acids such as oleic acid can inhibit osteoclast activity via Peroxisome Proliferator-Activated Receptor (PPAR) signaling [16,32]. In this study, exogenous oleic acid partially rescued osteoclast differentiation and resorption under SREBP1 inhibition (Figs. 4,5). These results suggest that SREBP1-mediated endogenous fatty acid synthesis regulates intracellular lipid composition and affects energy status, membrane structure, and fusion capacity,

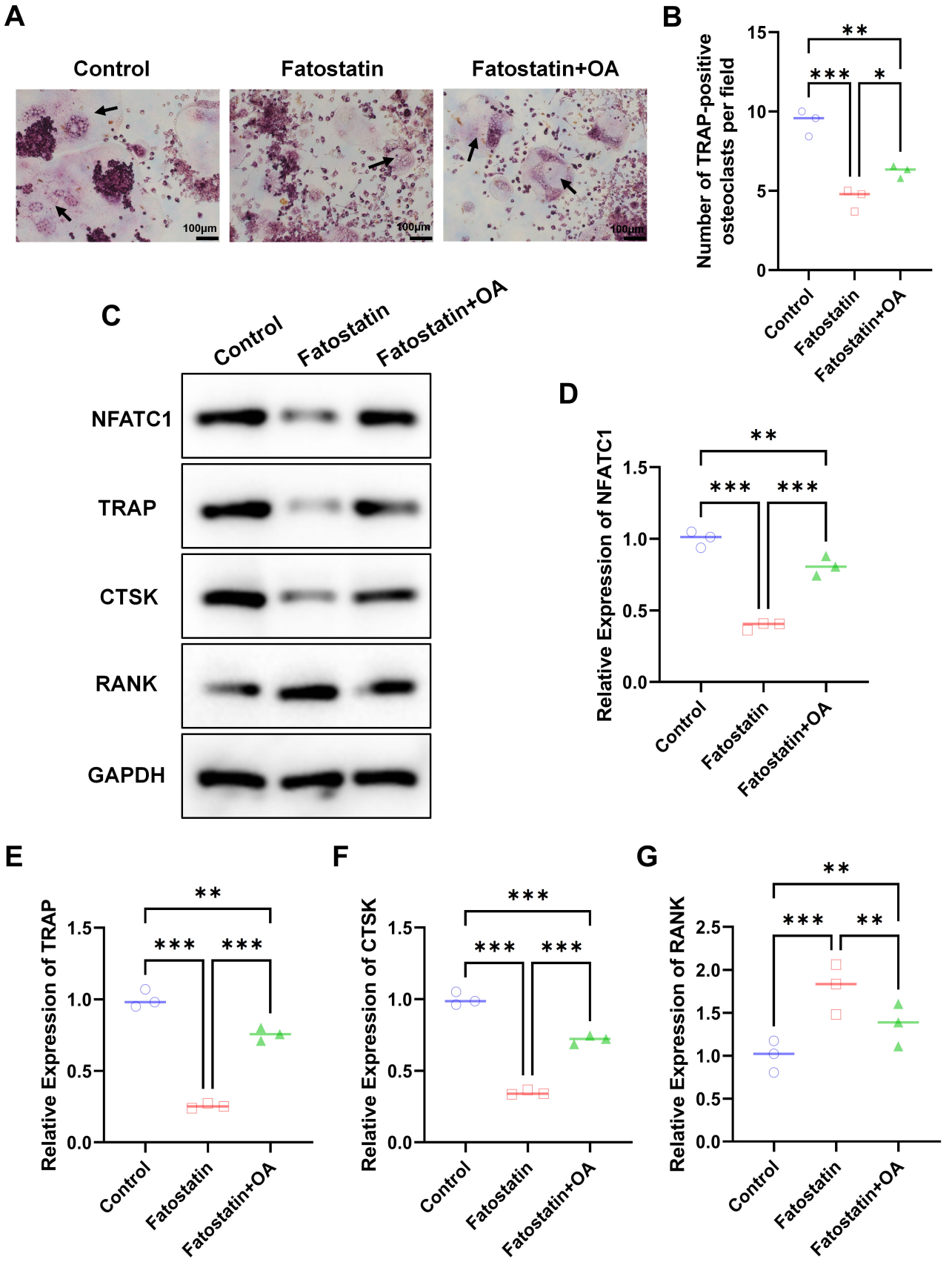

Fig. 5. Osteoclast differentiation and associated protein expression. (A) TRAP staining. (B) Quantification of TRAP-positive cells (Only TRAP-positive multinucleated osteoclasts were counted). (C–G) Western blot analysis and densitometry of NFATC1, TRAP, CTSK, and RANK. Arrows indicate positive cells. n = 3; *$p < 0.05$; **$p < 0.01$; ***$p < 0.001$.

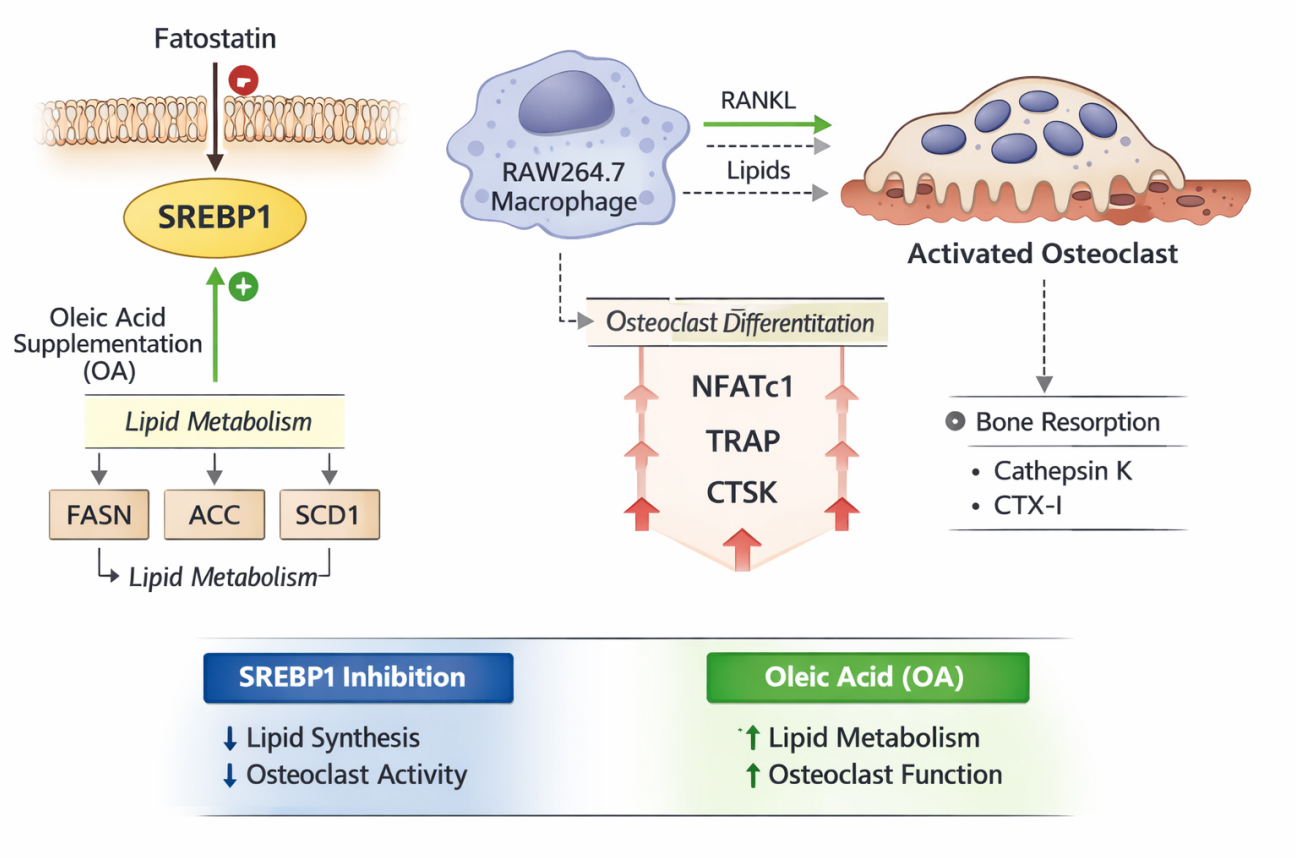

Fig. 6. Mechanistic model of SREBP1 in osteoclast lipid metabolism and function. The schematic diagram was created using WPS PowerPoint. Fatostatin-mediated inhibition of SREBP1 suppresses lipid metabolism-related enzymes (FASN, ACC, and SCD1), thereby reducing osteoclast differentiation and bone resorption, whereas OA partially restores lipid metabolism and osteoclast function. Solid arrows indicate regulatory relationships supported by the present study (Figs. 2,3,4,5). Dashed arrows represent potential or literature-based interactions that were not directly tested in this study, including the association between SREBP1-mediated lipid metabolism and NFATC1-driven osteoclast differentiation.

ultimately influencing bone resorption. Mechanistically, SREBP1 may provide lipid substrates for osteoclast fusion or modulate lipid-derived signaling molecules to control metabolism, consistent with previous studies [27,28].

Coupling of SREBP1-Lipid Metabolism and Bone Homeostasis under Estrogen Deficiency

Estrogen deficiency drives postmenopausal osteoporosis and induces lipid metabolic abnormalities [4]. OVX animals show upregulation of SREBP1c in the liver and peripheral tissues [33]. In our study, OVX mice exhibited reduced bone mechanical properties, increased osteoclast activity, and upregulated SREBP1 signaling in bone marrow (Figs. 1,2). This suggests SREBP1 as a critical node linking lipid metabolic remodeling to pathological bone resorption under estrogen-deficient conditions, supporting the notion that lipid dysregulation contributes to osteoporosis [27].

Mechanistic Insights and Therapeutic Implications

SREBP1 regulates osteoclast differentiation via lipid metabolic enzymes, including FASN, ACC, and SCD1, and exogenous fatty acids can partially restore osteoclast function. This highlights osteoclast-intrinsic lipid metabolism as a therapeutic target. SREBP inhibitors have been explored in cancer and metabolic disorders [34,35], and our study extends this concept to bone metabolism. Collectively, these findings are summarized in a mechanistic model illustrating how SREBP1-mediated lipid metabolic remodeling regulates osteoclast differentiation and function (Fig. 6). Clinically, potential strategies include osteoclast-targeted SREBP1 modulators, combination therapy with anti-resorptive agents, or fatty acid-based metabolic interventions. Adjusting fatty acid profiles may complement standard therapies and provide a “metabolism-bone” approach. Future studies should define upstream and downstream SREBP1 signaling and quantify the effects of fatty acid type, chain length, and saturation on osteoclast function.

Limitations and Future Directions

Despite the comprehensive *in vivo* and *in vitro* models used in this study, several limitations should be acknowledged. First, intracellular fatty acid composition and lipidomic profiles were not directly measured. Therefore, the proposed lipid metabolic remodeling is inferred primarily from the expression of lipid metabolism–related regulatory proteins rather than direct lipidomic evidence. Second, although osteoclast-specific gene manipulation using the Ctsk-Cre system has been widely reported, its cell-type specificity was not independently validated in the present study. Future studies could address this limitation using lineage-tracing approaches or additional cell-specific markers to confirm osteoclast lineage targeting and exclude potential off-target recombination. In addition, multicellular interactions within the osteoblast lineage and the periosteal microenvironment were not fully explored, and validation using human samples was not performed. Future work should incorporate quantitative lipidomics, metabolic flux analysis, single-cell metabolic profiling, and clinical sample validation to further clarify osteoclast–osteoblast coupling and signaling interactions with marrow adipocytes, thereby supporting the potential clinical translation of SREBP1-targeted strategies.

Conclusion

In summary, this study demonstrates that SREBP1-mediated lipid metabolic remodeling plays a pivotal role in osteoclast differentiation and bone resorption. SREBP1 and its downstream lipogenic enzymes were upregulated in OVX-induced osteoporosis and during RANKL-induced osteoclastogenesis, whereas genetic or pharmacological inhibition of SREBP1 significantly suppressed osteoclast formation and resorptive activity. Mechanistically, SREBP1 appears to facilitate osteoclast maturation by regulating fatty acid synthesis and supporting NFATC1 activation, while exogenous oleic acid partially rescues the functional deficits caused by SREBP1 inhibition. These findings identify SREBP1 as a key metabolic regulator of bone remodeling and suggest that targeting SREBP1-driven lipid metabolism may represent a potential therapeutic strategy for osteoporosis and related metabolic bone disorders.

Availability of Data and Materials

The datasets used or analyzed during the current study are available from the corresponding author upon reasonable request.

Author Contributions

XL contributed to the study conceptualization, methodology design, data analysis, and drafting of the original manuscript. BL participated in the investigation, data collection, data curation, and contributed to drafting and revising the manuscript for important intellectual content. FL provided methodological support, assisted with data interpretation and visualization, and was involved in drafting and critically revising the manuscript. NZ contributed to the study conceptualization and design, and was responsible for supervision, project administration, and manuscript review and editing. All authors have read and approved the final manuscript. All authors have participated sufficiently in the work to take public responsibility for appropriate portions of the content and agreed to be accountable for all aspects of the work in ensuring that questions related to its accuracy or integrity.

Ethics Approval and Consent to Participate

All animal experiments were approved by the Animal Ethics Committee of South Zhejiang Institute of Radiation Medicine and Nuclear Technology Applications (ZFY20250896). All procedures were carried out in accordance with institutional ethical guidelines, with efforts made to minimize animal use and suffering. This study was conducted in compliance with the ARRIVE Guidelines 2.0. All efforts were made to minimize animal use and suffering.

Acknowledgment

Not applicable.

Funding

This research was funded by the Science and Technology Program of Wenzhou (Grant No. YC20250554).

Conflict of Interest

The authors declare no conflict of interest.

References

[1] Kim JH, Kim N. Regulation of NFATc1 in Osteoclast Differentiation. Journal of Bone Metabolism. 2014; 21: 233–241. https://doi.org/10.11005/jbm.2014.21.4.233.

[2] Kuroda Y, Hisatsune C, Nakamura T, Matsuo K, Mikoshiba K. Osteoblasts induce Ca^{2+} oscillation-independent NFATc1 activation during osteoclastogenesis. Proceedings of the National Academy of Sciences of the United States of America. 2008; 105: 8643–8648. https://doi.org/10.1073/pnas.0800642105.

[3] Kim H, Oh B, Park-Min KH. Regulation of Osteoclast Differentiation and Activity by Lipid Metabolism. Cells. 2021; 10: 89. https://doi.org/10.3390/cells10010089.

[4] Paquette A, Wang D, Jankowski M, Gutkowska J, Lavoie JM. Effects of ovariectomy on PPAR alpha, SREBP-1c, and SCD-1 gene expression in the rat liver. Menopause. 2008; 15: 1169–1175. https://doi.org/10.1097/gme.0b013e31817b8159.

[5] Menéndez-Gutiérrez MP, Rőszer T, Fuentes L, Núñez V, Escolano A, Redondo JM, *et al*. Retinoid X receptors orchestrate osteoclast differentiation and postnatal bone remodeling. The Journal of Clinical Investigation. 2015; 125: 809–823. https://doi.org/10.1172/JCI77186.

[6] Chu W, Peng W, Lu Y, Liu Y, Li Q, Wang H, *et al*. PRMT6 Epigenetically Drives Metabolic Switch from Fatty Acid Oxida-

tion toward Glycolysis and Promotes Osteoclast Differentiation During Osteoporosis. Advanced Science. 2024; 11: e2403177. https://doi.org/10.1002/advs.202403177.

[7] Xiu C, Zhang L, Zhang C, Zhang Y, Luo X, Zhang Z, *et al*. Pharmacologically targeting fatty acid synthase-mediated de novo lipogenesis alleviates osteolytic bone loss by directly inhibiting osteoclastogenesis through suppression of STAT3 palmitoylation and ROS signaling. Metabolism: Clinical and Experimental. 2025; 167: 156186. https://doi.org/10.1016/j.metabol.2025.156186.

[8] Kamisuki S, Mao Q, Abu-Elheiga L, Gu Z, Kugimiya A, Kwon Y, *et al*. A small molecule that blocks fat synthesis by inhibiting the activation of SREBP. Chemistry & Biology. 2009; 16: 882–892. https://doi.org/10.1016/j.chembiol.2009.07.007.

[9] Brovkovych V, Izhar Y, Danes JM, Dubrovskyi O, Sakallioglu IT, Morrow LM, *et al*. Fatostatin induces pro- and anti-apoptotic lipid accumulation in breast cancer. Oncogenesis. 2018; 7: 66. https://doi.org/10.1038/s41389-018-0076-0.

[10] Li Y, Wu S, Zhao X, Hao S, Li F, Wang Y, *et al*. Key events in cancer: Dysregulation of SREBPs. Frontiers in Pharmacology. 2023; 14: 1130747. https://doi.org/10.3389/fphar.2023.1130747.

[11] Inoue K, Imai Y. Fatostatin, an SREBP inhibitor, prevented RANKL-induced bone loss by suppression of osteoclast differentiation. Biochimica et Biophysica Acta. 2015; 1852: 2432–2441. https://doi.org/10.1016/j.bbadis.2015.08.018.

[12] Kim H, Choi IA, Umemoto A, Bae S, Kaneko K, Mizuno M, *et al*. SREBP2 restricts osteoclast differentiation and activity by regulating IRF7 and limits inflammatory bone erosion. Bone Research. 2024; 12: 48. https://doi.org/10.1038/s41413-024-00354-4.

[13] Wang X, Chen Y, Meng H, Meng F. SREBPs as the potential target for solving the polypharmacy dilemma. Frontiers in Physiology. 2024; 14: 1272540. https://doi.org/10.3389/fphys.2023.1272540.

[14] Li M, Zhang J, Tang J, Zhou C, Zhang G, Liu H, *et al*. Effects of Lipid Metabolites and Cross Organ Lipid Metabolism Regulation on Bone Homeostasis. Aging and Disease. 2025. https://doi.org/10.14336/AD.2025.0575. (online ahead of print)

[15] Kim HJ, Lee DK, Jin X, Che X, Choi JY. Oleoylethanolamide Exhibits GPR119-Dependent Inhibition of Osteoclast Function and GPR119-Independent Promotion of Osteoclast Apoptosis. Molecules and Cells. 2020; 43: 340–349. https://doi.org/10.14348/molcells.2020.2260.

[16] Choi IA, Umemoto A, Mizuno M, Park-Min KH. Bone metabolism - an underappreciated player. Npj Metabolic Health and Disease. 2024; 2: 12. https://doi.org/10.1038/s44324-024-00010-9.

[17] Lal S, Gunji S, Ahluwalia P, Kolhe R, Bollag WB, Hill WD, *et al*. Lipid metabolism in age-related musculoskeletal disorders: insights into sarcopenia and osteoporosis. BMC Biology. 2025; 23: 265. https://doi.org/10.1186/s12915-025-02383-9.

[18] Guo X, Yu X, Yao Q, Qin J. Early effects of ovariectomy on bone microstructure, bone turnover markers and mechanical properties in rats. BMC Musculoskeletal Disorders. 2022; 23: 316. https://doi.org/10.1186/s12891-022-05265-1.

[19] Hsu SH, Chen LR, Chen KH. Primary Osteoporosis Induced by Androgen and Estrogen Deficiency: The Molecular and Cellular Perspective on Pathophysiological Mechanisms and Treatments. International Journal of Molecular Sciences. 2024; 25: 12139. https://doi.org/10.3390/ijms252212139.

[20] Das BK, Wang L, Fujiwara T, Zhou J, Aykin-Burns N, Krager KJ, *et al*. Transferrin receptor 1-mediated iron uptake regulates bone mass in mice via osteoclast mitochondria and cytoskeleton. eLife. 2022; 11: e73539. https://doi.org/10.7554/eLife.73539.

[21] Zheng X, Wang J, Bi F, Li Y, Xiao J, Chai Z, *et al*. Protective effects of *Lycium barbarum* polysaccharide on ovariectomy-induced cognition reduction in aging mice. International Journal of Molecular Medicine. 2021; 48: 121. https://doi.org/10.3892/ijmm.2021.4954.

[22] Ochiai S, Nishida Y, Higuchi Y, Morita D, Makida K, Seki T, *et al*. Short-range UV-LED irradiation in postmenopausal osteoporosis using ovariectomized mice. Scientific Reports. 2021; 11: 7875. https://doi.org/10.1038/s41598-021-86730-0.

[23] Tsubaki M, Takeda T, Matsuda T, Yamamoto Y, Higashinaka A, Yamamoto K, *et al*. Interleukin 19 suppresses RANKL-induced osteoclastogenesis via the inhibition of NF-κB and p38MAPK activation and c-Fos expression in RAW264.7 cells. Cytokine. 2021; 144: 155591. https://doi.org/10.1016/j.cyto.2021.155591.

[24] van Heerden B, Kasonga A, Kruger MC, Coetzee M. Palmitoleic Acid Inhibits RANKL-Induced Osteoclastogenesis and Bone Resorption by Suppressing NF-κB and MAPK Signalling Pathways. Nutrients. 2017; 9: 441. https://doi.org/10.3390/nu9050441.

[25] Han H, Li R, Fu D, Zhou H, Zhan Z, Wu Y, *et al*. Correlation between bone density, bone metabolism markers with lipid metabolism markers and body mass index. BMC Musculoskeletal Disorders. 2024; 25: 162. https://doi.org/10.1186/s12891-024-07284-6.

[26] Wang X, Zhang C, Zhao G, Yang K, Tao L. Obesity and lipid metabolism in the development of osteoporosis (Review). International Journal of Molecular Medicine. 2024; 54: 61. https://doi.org/10.3892/ijmm.2024.5385.

[27] Zhang J, Hu W, Zou Z, Li Y, Kang F, Li J, *et al*. The role of lipid metabolism in osteoporosis: Clinical implication and cellular mechanism. Genes & Diseases. 2023; 11: 101122. https://doi.org/10.1016/j.gendis.2023.101122.

[28] Ledesma-Colunga MG, Passin V, Lademann F, Hofbauer LC, Rauner M. Novel Insights into Osteoclast Energy Metabolism. Current Osteoporosis Reports. 2023; 21: 660–669. https://doi.org/10.1007/s11914-023-00825-3.

[29] Li N, Li X, Ding Y, Liu X, Diggle K, Kisseleva T, *et al*. SREBP Regulation of Lipid Metabolism in Liver Disease, and Therapeutic Strategies. Biomedicines. 2023; 11: 3280. https://doi.org/10.3390/biomedicines11123280.

[30] Xu X, Jin W, Chang R, Ding X. Research progress of SREBP and its role in the pathogenesis of autoimmune rheumatic diseases. Frontiers in Immunology. 2024; 15: 1398921. https://doi.org/10.3389/fimmu.2024.1398921.

[31] Kim H, Choi IA, Bae S, Kaneko K, Giannopoulou E, Deng L, *et al*. POS0418 SREBP2 REGULATES OSTEOCLAST DIFFERENTIATION AND PROTECTS MICE FROM INFLAMMATORY BONE LOSS. Annals of the Rheumatic Diseases. 2023; 82: 465. https://doi.org/10.1136/annrheumdis-2023-eular.5230.

[32] Kasonga AE, Kruger MC, Coetzee M. Free fatty acid receptor 4-β-arrestin 2 pathway mediates the effects of different classes of unsaturated fatty acids in osteoclasts and osteoblasts. Biochimica et Biophysica Acta. Molecular and Cell Biology of Lipids. 2019; 1864: 281–289. https://doi.org/10.1016/j.bbalip.2018.12.009.

[33] Dong J, Dennis KMJH, Venkatakrishnan R, Hodson L, Tomlinson JW. The Impact of Estrogen Deficiency on Liver Metabolism: Implications for Hormone Replacement Therapy. Endocrine Reviews. 2025; 46: 790–809. https://doi.org/10.1210/endrev/bnaf018.

[34] Hajirahimkhan A, Brown KA, Clare SE, Khan SA. SREBP1-Dependent Metabolism as a Potential Target for Breast Cancer Risk Reduction. Cancers. 2025; 17: 1664. https://doi.org/10.3390/cancers17101664.

[35] Terry AR, Hay N. Emerging targets in lipid metabolism for cancer therapy. Trends in Pharmacological Sciences. 2024; 45: 537–551. https://doi.org/10.1016/j.tips.2024.04.007.